Fluctuation driven topological transition of binary condensates in optical lattices

K. Suthar,[1,2] Arko Roy,[1,2] and D. Angom[1]

[1] *Physical Research Laboratory, Navrangpura, Ahmedabad-380009, Gujarat, India*
[2] *Indian Institute of Technology, Gandhinagar, Ahmedabad-382424, Gujarat, India*

(Dated: December 2, 2014)

We show the emergence of a third Goldstone mode in binary condensates at the phase-separation in quasi-1D optical lattices. We develop the coupled discrete nonlinear Schrödinger equations (DNLSEs) using Hartree-Fock-Bogoliubov theory with Popov approximation in the Bose-Hubbard model to investigate the mode evolution at zero temperature. In particular, as the system is driven from miscible to immiscible phase. We demonstrate that the position swapping of the species in ^{87}Rb-^{85}Rb system is accompanied by a discontinuity in the excitation spectrum. Our results show that in quasi-1D optical lattices, the presence of the fluctuations dramatically change the geometry of the ground state density profile of TBEC.

PACS numbers: 42.50.Lc, 67.85.Bc, 67.85.Fg, 67.85.Hj

arXiv:1412.0405v1 [cond-mat.quant-gas] 1 Dec 2014

I. INTRODUCTION

Ultracold dilute atomic Bose gases in low dimensions have been the subject of growing interest over the last few decades. These are an ideal platform to probe many-body phenomena where quantum fluctuations play a crucial role [1, 2]. In particular, the use of optical lattices serve as an excellent and versatile tool to study the physics of strongly correlated systems, and other phenomena in condensed matter physics [3, 4]. A variety of experimental techniques have been used to load and manipulate Bose-Einstein condensates (BECs) in optical lattices [5–8]. These have helped to explore quantum phase transition [9] namely superfluid (SF)–Mott insulator (MI) transition [10–13]. The characteristics of SF phase, such as coherence [14, 15], collective modes [16] and transport [17, 18] have also been observed. The center of mass dipole oscillation of BEC in a cigar-shaped lattice potential has been experimentally studied in detail [19]. In such systems, a decrease in the Kohn mode frequency has been reported in Ref. [20] which has been justified in Ref. [21] as the increase of the effective mass due to the lattice potential. On the theoretical front, the low-lying collective excitations of a trapped Bose gas in periodic lattice potential have been studied in Refs. [22–25] using Bose-Hubbard (BH) model [26].

The two-component BEC (TBEC), on the other hand, exhibits an unique property that they can be phase-separated [27]. There have been numerous experimental and theoretical investigations of binary mixtures of BECs over the last few years. Experimentally, it is possible to vary the interactions through Feshbach resonance [28, 29], and drive the binary mixture from miscible to immiscible phase or vice-versa. Among the various lines of investigation, the theoretical study of the stationary states [30], dynamical instabilities [31, 32] and the collective excitations [33, 34] of TBECs are noteworthy. Furthermore, in optical lattices TBECs have also been observed in recent experiments [35, 36].Theoretical studies of TBECs in optical lattices [37–40] and, in particular, phase-separation [41–43] and dynamical instabilities [44] have also been carried out. Despite all these theoretical and experimental advancements, the study of collective excitations of TBECs in optical lattices is yet to be explored. This is the research gap addressed in the present work.

In this paper, we report the development of coupled discrete nonlinear Schrödinger equations (DNLSEs) of TBECs in optical lattices under Hartree-Fock-Bogoliubov-Popov approximation [45]. We use this theory to study the ground state density-profiles and the quasiparticle spectrum of ^{87}Rb-^{85}Rb and ^{133}Cs-^{87}Rb TBECs at zero temperature. We, in particular, focus on the evolution of the quasiparticle as the TBEC is driven from miscible to immiscible phase. This is possible by the tuning either the intra- or interspecies interaction strengths. The two systems considered correspond to these possibilities. The fluctuation and interaction induced effect on the collective excitation spectra and topological change in density profiles is the major finding of our present study. It deserves to be mentioned here that for systems without the lattice potential, at equilibrium, recent works have shown the existence of additional Goldstone modes in TBECs at phase-separation [46] and complex eigenenergies due to quantum fluctuations [47].

The paper is organized as follows. Sec. II describes the tight-binding approximation for a trapped BEC in 1D lattice potential. In Sec. III we present the HFB-Popov theory to determine the quasiparticle energies and mode functions of single component BEC and TBECs at finite temperature. The results of our studies are presented in Sec. IV. Finally, we highlight the key results of our work in Sec. V.

II. QUASI-1D OPTICAL LATTICE

We consider a Bose-Einstein condensate (BEC), held within a highly anisotropic cigar shaped harmonic potential with trapping frequencies $\omega_x = \omega_y = \omega_\perp \gg \omega_z$. In this case we can integrate out the condensate wavefunction along x and y-direction and reduce it to a quasi-

1D condensate. In the mean-field approximation, the grand-canonical Hamiltonian, in the second quantized form, of the bosonic atoms in an external potential plus lattice is given by

$$\begin{aligned}\hat{H} = & \int dz\hat{\Psi}^\dagger(z)\left(-\frac{\hbar^2}{2m}\frac{\partial^2}{\partial z^2}+V_{\rm latt}(z)\right)\hat{\Psi}(z)\\ &+\int dz(V_{\rm ext}-\mu)\hat{\Psi}^\dagger(z)\hat{\Psi}(z)\\ &+\frac{1}{2}\int dzdz'\hat{\Psi}^\dagger(z)\hat{\Psi}^\dagger(z')U(z-z')\hat{\Psi}(z)\hat{\Psi}(z'), \quad (1)\end{aligned}$$

where $\hat{\Psi}(z)$ and $\hat{\Psi}^\dagger(z)$ are the bosonic field operators which obey the Bose commutation relations, m is the atomic mass of the species, $V_{\rm latt}$ is the periodic lattice potential, $V_{\rm ext}$ is the external trapping potential, μ is the chemical potential and $U = 2\sqrt{\lambda\kappa}\hbar^2 N a_s/m$, with N as the total number of atoms, $\lambda = \omega_x/\omega_z$ and $\kappa = \omega_y/\omega_z$ are the anisotropy parameters along x- and y-direction, and a_s as the s-wave scattering length, which is repulsive ($a_s > 0$) in the present work. The net external potential is

$$\begin{aligned}V &= V_{\rm ext} + V_{\rm latt}\\ &= \frac{1}{2}m\omega_z^2 z^2 + V_0\sin^2(kz), \quad (2)\end{aligned}$$

where $V_0 = sE_R$ is the optical lattice depth with s and E_R as the lattice depth scaling parameter, and the recoil energy of the laser light photon, respectively. The wave number of the counter-propagating laser beams, which are used to create periodic lattice potential is $k = \pi/a$ with $a = \lambda_L/2$ is the lattice spacing and λ_L is the wavelength of the laser light. The energy barrier between adjacent lattice sites is expressed in units of the recoil energy $E_R = \hbar^2k^2/2m$. In tight binding approximation, valid when $\mu \ll V_0$, the 1D field operator can be written as [48]

$$\hat{\Psi}(z) = \sum_j \hat{a}_j\phi_j(z), \quad (3)$$

where $\hat{a}_j$ is the annihilation operator corresponding to the jth site, and the spatial part $\phi_j(z) = \phi(z - ja)$ is the orthonormal Gaussian orbital of the lowest vibrational band centered at the jth lattice site, with $\int dz\ \phi^*_{j\pm1}(z)\phi_j(z) = 0$ and $\int dz\ |\phi_j(z)|^2 = 1$. By using above ansatz in $\hat{H}$ and considering only the nearest neighbour tunneling we obtain the Bose-Hubbard (BH) Hamiltonian.

III. HFB-POPOV APPROXIMATION

A. Single-component BEC in optical lattices

The BH Hamiltonian describes the dynamics of 1D optical lattices when only the lowest band or the lowest vibrational level of the site is occupied. In this case the tight binding approximation [49] is valid, and the BH Hamiltonian of the system is

$$\hat{H} = -J\sum_{\langle jj'\rangle}\hat{a}_j^\dagger\hat{a}_{j'} + \sum_j\left[(\epsilon_j-\mu)\hat{a}_j^\dagger\hat{a}_j + \frac{1}{2}U\hat{a}_j^\dagger\hat{a}_j^\dagger\hat{a}_j\hat{a}_j\right], \quad (4)$$

where the index j runs over the lattice sites, $\langle jj'\rangle$ represents the nearest neighbour sum, and $\hat{a}_j(\hat{a}_j^\dagger)$ is the bosonic annihilation (creation) operator of a bosonic atom at the jth lattice site. Here $J = \int dz\ \phi^*_{j+1}(z)[-(\hbar^2/2m)(\partial^2/\partial z^2) + V_0\sin^2(2\pi z/\lambda_L)]\phi_j(z)$ is the tunneling matrix element between adjacent sites, $\epsilon_j = \int dz\ V_{\rm ext}(z)|\phi_j(z)|^2$ is the energy offset of the jth lattice site, and $U = (2\sqrt{\lambda\kappa}\hbar^2 N a_s/m)\int dz|\phi_j(z)|^4$ is the on-site interaction strength of atoms occupying the jth lattice site. The offset energy can also be expressed as $\epsilon_j = j^2\Omega$, here, $\Omega = m\omega_z^2a^2/2$ is the energy cost to move a boson from the central site to its nearest neighbour site. To take into account the quantum fluctuations and thermal effects in the description of the system, we decompose the Bose field operator of each lattice site j in terms of a complex mean-field part c_j and a fluctuation operator $\hat{\varphi}_j$, as $\hat{a}_j = (c_j + \hat{\varphi}_j)e^{-i\mu t/\hbar}$. Using this field operator in the BH Hamiltonian, we get

$$\hat{H} = H_0 + \hat{H}_1 + \hat{H}_2 + \hat{H}_3 + \hat{H}_4, \quad (5)$$

with

$$H_0 = -J\sum_{\langle jj'\rangle}c_j^*c_{j'} + \sum_j\left[(\epsilon_j-\mu)|c_j|^2 + \frac{1}{2}U|c_j|^4\right], \quad (6a)$$

$$\hat{H}_1 = -J\sum_{\langle jj'\rangle}\hat{\varphi}_jc_{j'}^* + \sum_j\left(\epsilon_j-\mu+U|c_j|^2\right)c_j^*\hat{\varphi}_j + \text{h.c.}, \quad (6b)$$

$$\begin{aligned}\hat{H}_2 = &-J\sum_{\langle jj'\rangle}\hat{\varphi}_j^\dagger\hat{\varphi}_{j'} + \sum_j(\epsilon_j-\mu)\hat{\varphi}_j^\dagger\hat{\varphi}_j\\ &+\frac{U}{2}\sum_j\left(\hat{\varphi}_j^{\dagger2}c_j^2 + \hat{\varphi}_j^2c_j^{*2} + 4|c_j|^2\hat{\varphi}_j^\dagger\hat{\varphi}_j\right), \quad (6c)\end{aligned}$$

$$\hat{H}_3 = U\sum_j\hat{\varphi}_j^\dagger\hat{\varphi}_j^\dagger\hat{\varphi}_jc_j + \text{h.c.}, \quad (6d)$$

$$\hat{H}_4 = \frac{U}{2}\sum_j\hat{\varphi}_j^\dagger\hat{\varphi}_j^\dagger\hat{\varphi}_j\hat{\varphi}_j, \quad (6e)$$

where subscript of the various terms indicates the order of fluctuation operators and h.c. stands for the hermitian conjugate. To study the system without quantum fluctuation at $T = 0K$, we consider terms up to second order in $\hat{\varphi}_j$ and neglect the higher order terms (third and fourth order). The lowest order term of the Hamiltonian describes the condensate part of the system. The minimization of H_0 with respect to the variation in the complex amplitude c_j^* gives the time independent DNLSE,

which can be written as

$$\mu c_j = -J(c_{j-1} + c_{j+1}) + (\epsilon_j + Un_j^c)c_j, \tag{7}$$

with the condensate density $n_j^c = |c_j|^2$. The quadratic Hamiltonian $\hat{H}_2$ is the leading order term which describes the noncondensate part, since the variation in $\hat{H}_1$ vanishes by using the fact that c_j is a stationary solution of the DNLSE. The minimization of $\hat{H}_2$ yields the governing equation for the noncondensate given by

$$\mu\hat{\varphi}_j = -J(\hat{\varphi}_{j-1} + \hat{\varphi}_{j+1}) + (\epsilon_j + 2Un_j^c)\hat{\varphi}_j + Uc_j^2\hat{\varphi}_j^\dagger. \tag{8}$$

The quadratic Hamiltonian can be diagonalized using the Bogoliubov transformation

$$\hat{\varphi}_j = \sum_l \left[u_j^l\hat{\alpha}_l e^{-i\omega_l t} - v_j^{*l}\hat{\alpha}_l^\dagger e^{i\omega_l t}\right], \tag{9a}$$

$$\hat{\varphi}_j^\dagger = \sum_l \left[u_j^{*l}\hat{\alpha}_l^\dagger e^{i\omega_l t} - v_j^l\hat{\alpha}_l e^{-i\omega_l t}\right], \tag{9b}$$

where u_j^l and v_j^l are the quasiparticle amplitudes, $\omega_l = E_l/\hbar$ is the lth quasiparticle mode frequency with E_l as the mode energy, and $\hat{\alpha}_l(\hat{\alpha}_l^\dagger)$ are the quasiparticle annihilation (creation) operators, which satisfy the Bose commutation relations. The quasiparticle amplitudes satisfy the following normalization conditions

$$\sum_j \left(u_j^{*l}u_j^{l'} - v_j^{*l}v_j^{l'}\right) = \delta_{ll'}, \tag{10a}$$

$$\sum_j \left(u_j^l v_j^{l'} - v_j^{*l}u_j^{*l'}\right) = 0. \tag{10b}$$

By using the definitions of $\hat{\varphi}_j$ from Eq. (9) in $\hat{H}_2$ [Eq. (6c)] and using the above conditions, we get the following Bogoliubov-de Gennes (BdG) equations

$$E_l u_j^l = -J(u_{j-1}^l + u_{j+1}^l) + [2Un_j^c + (\epsilon_j - \mu)]u_j^l - Uc_j^2 v_j^l, \tag{11a}$$

$$E_l v_j^l = J(v_{j-1}^l + v_{j+1}^l) - [2Un_j^c + (\epsilon_j - \mu)]v_j^l + Uc_j^{*2}u_j^l. \tag{11b}$$

This set of coupled equations describe the quasiparticles of condensate in the optical lattice without considering the quantum fluctuations.

To investigate the effect of fluctuation and finite temperature we include the higher order terms ($\hat{H}_3$ and $\hat{H}_4$) of the fluctuation operator in the Hamiltonian. We treat these terms in the self-consistent mean-field approximation [45] such that $\hat{\varphi}_j^\dagger\hat{\varphi}_j\hat{\varphi}_j \approx 2\tilde{n}_j\hat{\varphi}_j + \tilde{m}_j\hat{\varphi}_j^\dagger$ and $\hat{\varphi}_j^\dagger\hat{\varphi}_j^\dagger\hat{\varphi}_j\hat{\varphi}_j \approx 4\tilde{n}_j\hat{\varphi}_j^\dagger\hat{\varphi}_j + \tilde{m}_j\hat{\varphi}_j^\dagger\hat{\varphi}_j^\dagger + \tilde{m}_j^*\hat{\varphi}_j\hat{\varphi}_j - (2\tilde{n}_j^2 + |\tilde{m}_j|^2)$, where $\tilde{n}_j = \langle\hat{\varphi}_j^\dagger\hat{\varphi}_j\rangle$ and $\tilde{m}_j = \langle\hat{\varphi}_j\hat{\varphi}_j\rangle$ are the excited population (noncondensate) density and anomalous density at the jth site, respectively. In the HFB-Popov approximation, where the anomalous density is neglected, the corrections from higher order terms yield the modified DNLSE

$$\mu' c_j = -J(c_{j-1} + c_{j+1}) + [\epsilon_j + U(n_j^c + 2\tilde{n}_j)]c_j, \tag{12}$$

where μ' is the modified chemical potential. The total density is $n = \sum_j(n_j^c + \tilde{n}_j)$. The diagonalization of the modified Hamiltonian leads to the following HFB-Popov equations

$$E_l u_j^l = -J(u_{j-1}^l + u_{j+1}^l) + [2U(n_j^c + \tilde{n}_j) + (\epsilon_j - \mu')]u_j^l - Uc_j^2 v_j^l, \tag{13a}$$

$$E_l v_j^l = J(v_{j-1}^l + v_{j+1}^l) - [2U(n_j^c + \tilde{n}_j) + (\epsilon_j - \mu')]v_j^l + Uc_j^{*2}u_j^l, \tag{13b}$$

with the noncondensate density at the jth lattice site given by

$$\tilde{n}_j = \sum_l [(|u_j^l|^2 + |v_j^l|^2)N_0(E_l) + |v_j^l|^2], \tag{14}$$

where $N_0(E_l) = \langle\hat{\alpha}_l^\dagger\hat{\alpha}_l\rangle = (e^{\beta E_l} - 1)^{-1}$ is the Bose-Einstein distribution function of the quasiparticle state with real and positive mode energy E_l. The coupled Eqs. (12) and (13) are solved iteratively until the solutions converge to desired accuracy. It is important to note that, at $T = 0K$, $N_0(E_l)$ in the above equation vanishes. The noncondensate density, then, has contribution from only the quantum fluctuations, which is given by

$$\tilde{n}_j = \sum_l |v_j^l|^2. \tag{15}$$

Therefore, we solve the equations self-consistently in the presence of the quantum fluctuations.

B. Two-component BEC in optical lattices

For two species condensate, the 1D second quantized grand canonical Hamiltonian is given by

$$\hat{H} = \sum_{i=1}^{2}\int dz\hat{\Psi}_i^\dagger(z)\Big[-\frac{\hbar^2}{2m_i}\frac{\partial^2}{\partial z^2} + V^i(z) - \mu_i + \frac{U_{ii}}{2}\hat{\Psi}_i^\dagger(z) \times \hat{\Psi}_i(z)\Big]\hat{\Psi}_i(z) + U_{12}\int dz\hat{\Psi}_1^\dagger(z)\hat{\Psi}_2^\dagger(z)\hat{\Psi}_1(z)\hat{\Psi}_2(z), \tag{16}$$

where $i = 1, 2$ denotes the species index, $\hat{\Psi}_i$'s are the annihilation field operators for two different species, μ_i is the chemical potential of the ith species, U_{ii} are the intraspecies interaction parameters, and U_{12} is the interspecies interaction parameter with m_i's as the atomic masses of the species. Here, we consider repulsive interactions, $U_{ii}, U_{12} > 0$. The external potential V^i is the sum of harmonic and periodic optical lattice potential.

It is given by

$$V^i = V^i_{\rm ext} + V^i_{\rm latt} = \frac{1}{2}m_i\omega^2_{z_i}z_i^2 + V_0\sin^2(2\pi z_i/\lambda_L). \quad (17)$$

In the present work, we consider the same external potential for both the species. The depth of the lattice potential is also same for both species which is $V_0 = sE_R$ with $E_R = \hbar^2k^2/2m_1$. If the lattice is deep enough, the tight-binding approximation is valid, and the bosons can be assumed to occupy the lowest vibrational band only. Under this approximation, the Bose field operator for the two species can be expanded as

$$\hat{\Psi}_i(z) = \sum_j \hat{a}_{ij}\phi_{ij}(z), \quad (18)$$

where $\hat{a}_{ij}$'s are the annihilation operators and $\phi_{ij}(z)$'s are the orthonormal Gaussian basis of the two species. For the present work we assume that the width of the Gaussian basis are identical for both the species ($\phi_{1j} = \phi_{2j}$). The BH Hamiltonian for two species can be obtained by using the above ansatz in the Hamiltonian, Eq. (16). We, then, obtain the many-body Hamiltonian governing the system of binary BEC in quasi-1D optical lattice as

$$\hat{H} = \sum_{i=1}^{2}\left[-\sum_{\langle jj'\rangle} J_i\hat{a}^\dagger_{ij}\hat{a}_{ij'} + \sum_j(\epsilon^{(i)}_j - \mu_i)\hat{a}^\dagger_{ij}\hat{a}_{ij}\right] + \frac{1}{2}\sum_{i=1}^{2}U_{ii}\sum_j\hat{a}^\dagger_{ij}\hat{a}^\dagger_{ij}\hat{a}_{ij}\hat{a}_{ij} + U_{12}\sum_j\hat{a}^\dagger_{1j}\hat{a}_{1j}\hat{a}^\dagger_{2j}\hat{a}_{2j}. \quad (19)$$

Here J_i are the tunneling matrix elements, and $\epsilon^{(i)}_j$ is the offset energy of species i at the jth lattice site. In the mean-field approximation, using Bogoliubov approximation like in single species condensate we decompose the operators of both species as $\hat{a}_{1j} = (c_j + \hat{\varphi}_{1j})e^{-i\mu_1 t/\hbar}$ and $\hat{a}_{2j} = (d_j + \hat{\varphi}_{2j})e^{-i\mu_2 t/\hbar}$. We use these definitions in the BH Hamiltonian [Eq. (19)] and then decompose the Hamiltonian into different terms according to the order of noncondensate operator they contain. The minimization of the lowest order term gives the stationary state equations or time-independent coupled DNLSEs, and these are given by

$$\mu_1 c_j = -J_1(c_{j-1} + c_{j+1}) + \left[\epsilon^{(1)}_j + U_{11}n^c_{1j} + U_{12}n^c_{2j}\right]c_j, \quad (20a)$$

$$\mu_2 d_j = -J_2(d_{j-1} + d_{j+1}) + \left[\epsilon^{(2)}_j + U_{22}n^c_{2j} + U_{12}n^c_{1j}\right]d_j, \quad (20b)$$

where $n^c_{1j} = |c_j|^2$ and $n^c_{2j} = |d_j|^2$ are the condensate densities of the first and second species, respectively. The noncondensate part of the TBEC is obtained by the minimization of the quadratic Hamiltonian

$$\mu_1\hat{\varphi}_{1j} = -J_1(\hat{\varphi}_{1,j-1} + \hat{\varphi}_{1,j+1}) + \left[\epsilon^{(1)}_j + 2U_{11}n^c_{1j}\right]\hat{\varphi}_{1j} + U_{11}c_j^2\hat{\varphi}^\dagger_{1j} + U_{12}(n^c_{2j}\hat{\varphi}_{1j} + d^*_jc_j\hat{\varphi}_{2j} + d_jc_j\hat{\varphi}^\dagger_{2j}), \quad (21a)$$

$$\mu_2\hat{\varphi}_{2j} = -J_2(\hat{\varphi}_{2,j-1} + \hat{\varphi}_{2,j+1}) + \left[\epsilon^{(2)}_j + 2U_{22}n^c_{2j}\right]\hat{\varphi}_{2j} + U_{22}d_j^2\hat{\varphi}^\dagger_{2j} + U_{12}(n^c_{1j}\hat{\varphi}_{2j} + c^*_jd_j\hat{\varphi}_{1j} + c_jd_j\hat{\varphi}^\dagger_{1j}). \quad (21b)$$

The Bogoliubov transformation equations of the TBEC, which couples the positive and negative energy mode excitations, are

$$\hat{\varphi}_{ij} = \sum_l\left[u^l_{ij}\hat{\alpha}_le^{-i\omega_lt} - v^{*l}_{ij}\hat{\alpha}^\dagger_le^{i\omega_lt}\right], \quad (22a)$$

$$\hat{\varphi}^\dagger_{ij} = \sum_l\left[u^{*l}_{ij}\hat{\alpha}^\dagger_le^{i\omega_lt} - v^l_{ij}\hat{\alpha}_le^{-i\omega_lt}\right], \quad (22b)$$

where u^l_{ij} and v^l_{ij} are the quasiparticle amplitudes for the first ($i = 1$) and second ($i = 2$) species. The above transformation diagonalizes the quadratic Hamiltonian and gives the Bogoliubov-de Gennes (BdG) equations at $T = 0K$ for the two-component system. The inclusion of the higher order terms of the perturbation or fluctuation in the quadratic Hamiltonian gives the HFB-Popov equations for the two-component BEC

$$E_lu^l_{1,j} = -J_1(u^l_{1,j-1} + u^l_{1,j+1}) + \mathcal{U}_1u^l_{1,j} - U_{11}c_j^2v^l_{1,j} + U_{12}c_j(d^*_ju^l_{2,j} - d_jv^l_{2,j}), \quad (23a)$$

$$E_lv^l_{1,j} = J_1(v^l_{1,j-1} + v^l_{1,j+1}) + \underline{\mathcal{U}}_1v^l_{1,j} + U_{11}c_j^{*2}u^l_{1,j} - U_{12}c^*_j(d_jv^l_{2,j} - d^*_ju^l_{2,j}), \quad (23b)$$

$$E_lu^l_{2,j} = -J_2(u^l_{2,j-1} + u^l_{2,j+1}) + \mathcal{U}_2u^l_{2,j} - U_{22}d_j^2v^l_{2,j} + U_{12}d_j(c^*_ju^l_{1,j} - c_jv^l_{1,j}), \quad (23c)$$

$$E_lv^l_{2,j} = J_2(v^l_{2,j-1} + v^l_{2,j+1}) + \underline{\mathcal{U}}_2v^l_{2,j} + U_{22}d_j^{*2}u^l_{2,j} - U_{12}d^*_j(c_jv^l_{1,j} - c^*_ju^l_{1,j}), \quad (23d)$$

where $\mathcal{U}_1 = 2U_{11}(n^c_{1j} + \tilde{n}_{1j}) + U_{12}(n^c_{2j} + \tilde{n}_{2j}) + (\epsilon^{(1)}_j - \mu_1)$, $\mathcal{U}_2 = 2U_{22}(n^c_{2j} + \tilde{n}_{2j}) + U_{12}(n^c_{1j} + \tilde{n}_{1j}) + (\epsilon^{(2)}_j - \mu_2)$ with $\underline{\mathcal{U}}_i = -\mathcal{U}_i$. The density of the noncondensate atoms at the jth lattice site is

$$\tilde{n}_{ij} = \sum_l[(|u^l_{ij}|^2 + |v^l_{ij}|^2)N_0(E_l) + |v^l_{ij}|^2], \quad (24)$$

with $N_0(E_l)$ as the Bose-factor of the system with energy E_l at temperature T. At $T = 0K$ the noncondensate part reduces to the quantum fluctuations

$$\tilde{n}_{ij} = \sum_l|v^l_{ij}|^2. \quad (25)$$

If we neglect quantum fluctuations (noncondensate part), the HFB-Popov Eqs. (23) are the BdG equations for bi-

nary BEC.

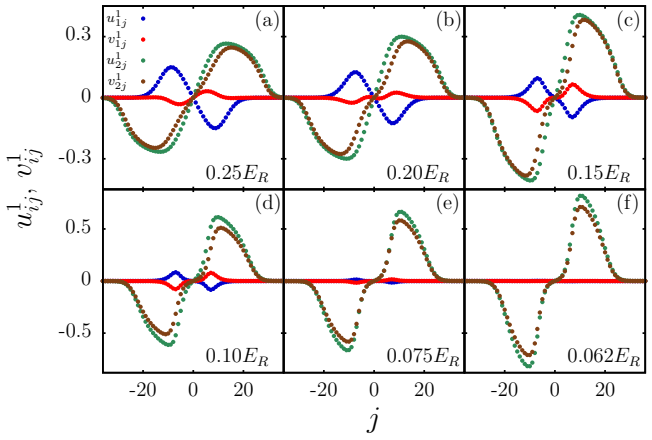

FIG. 1. The evolution of the quasiparticle amplitudes corresponding to the ^{85}Rb Kohn mode as the intraspecies interaction of ^{85}Rb (U_{22}) is decreased from $0.25E_R$ to $0.062E_R$. (a)-(b) When $U_{22} \geq 0.18E_R$, the system is in miscible phase and the Kohn mode ($l = 1$) have contributions from both the species, (c)-(e) when system is on the verge of the phase separation, then the Kohn mode of ^{85}Rb goes soft, and (f) at phase separation $U_{22} \leq 0.065E_R$ the Kohn mode transforms into a Goldstone mode.

IV. RESULTS AND DISCUSSIONS

A. Numerical details

We solve the scaled coupled DNLSE using fourth-order Runge-Kutta method to find the equilibrium state of the harmonically trapped binary condensates in optical lattices. We start the calculations for $T = 0$K by ignoring the quantum fluctuations at each lattice site. The initial complex amplitudes of both species c_j and d_j are chosen as $1/\sqrt{N_{\rm latt}}$, with $N_{\rm latt}$ as the total number of lattice sites. The advantage of this choice is that the amplitudes are normalized. We, then, use imaginary time propagation of the DNLSEs, Eqs. (20), to find the stationary ground state wave function of the TBEC. In the tight binding limit, the condensate wave function can be defined as the superposition of the basis functions as shown in Eq. (18). The basis function is chosen as the ground state, which is a Gaussian function, of lowest energy band [48]. The width of the function is a crucial parameter as it affects the overlap of the Gaussian orbitals at each lattice site. The correct estimation of the width is required in order to obtain orthonormal basis functions [50]. Furthermore, to study the excitation spectrum, we cast the Eqs. (23) as a matrix eigenvalue equation. The matrix is $4N_{\rm latt} \times 4N_{\rm latt}$, non-Hermitian, non-symmetric and may have complex eigenvalues. To diagonalize the matrix and to find the quasiparticle energies E_l, and amplitudes u^l_{ij}'s and v^l_{ij}'s, we use the routine ZGEEV from the LAPACK library [51]. In the later part of the work, when we include the effect of the quantum fluctuations, we need to solve Eqs. (20) and Eqs. (23) self-consistently. For this we iterate the solution until we reach desired convergence in the number of condensate and noncondensate atoms. In this process, sometimes, we encounter severe oscillations in the number of atoms. To damp these oscillations and accelerate convergence we employ a successive over (under) relaxation technique for updating the condensate (noncondensate) atom densities [52]. The new solutions after the iteration cycle (IC) are given by

$$c^{\rm new}_{j,{\rm IC}} = r^{\rm ov} c_{j,{\rm IC}} + (1 - r^{\rm ov}) c_{j,{\rm IC}-1}, \tag{26a}$$
$$\tilde{n}^{\rm new}_{j,{\rm IC}} = r^{\rm un} \tilde{n}_{j,{\rm IC}} + (1 - r^{\rm un}) \tilde{n}_{j,{\rm IC}-1}, \tag{26b}$$

where $r^{\rm ov} > 1$ ($r^{\rm un} < 1$) is the over (under) relaxation parameter. After the condensate and noncondensate density converge, we compute low-lying mode energies, and amplitude u^l_{ij}'s and v^l_{ij}'s. During computation, we ensure that the eigenvalues of the HFB-Popov matrix are real as there are no topological defects present in the system.

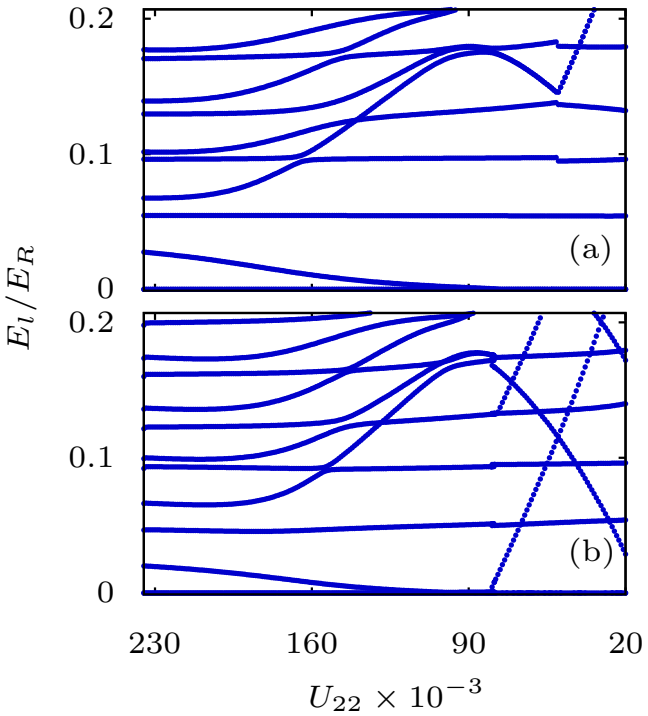

FIG. 2. The evolution of the low-lying modes as a function of the intraspecies interaction of the ^{85}Rb (U_{22}) in the ^{87}Rb-^{85}Rb TBEC held in quasi-1D optical lattices. (a) Excitation spectrum at zero temperature and (b) is the excitation spectrum in the presence of the quantum fluctuations. Here U_{22} is in units of the recoil energy E_R.

B. Mode evolution of trapped TBEC at $T = 0K$

Under the HFB-Popov approximation, the excitation spectrum of TBEC in optical lattice is gapless for the SF phase, while it has a finite gap for the MI phase [10]. In SF phase, the spontaneous symmetry breaking at condensation results in two Goldstone modes, one each for the two species. The number of Goldstone modes, however, depends on whether the system is in miscible or immiscible phase, and geometry of the density distributions. To explore different possibilities, as mentioned earlier, we consider two different TBEC systems. These are binary mixtures which can be driven from miscible to immiscible phase through the variation of intra- or interspecies interaction using Feshbach resonance. In particular, we consider ^{87}Rb - ^{85}Rb [28, 53] and ^{133}Cs - ^{87}Rb [54, 55] binary condensates as examples of the two cases, and study the mode evolution as the system approaches immiscible from miscible regime.

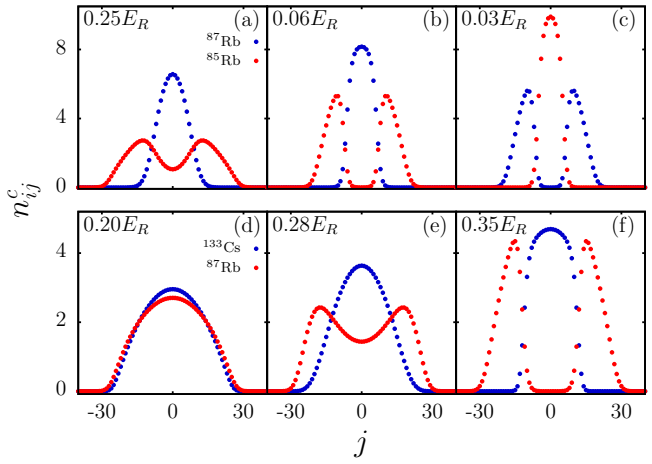

FIG. 3. The geometry of the condensate density profiles and its transition from miscible to the immiscible regime. (a-c) The transition from miscible to the *sandwich* profile for ^{87}Rb-^{85}Rb TBEC with the change in the intraspecies interaction U_{22} at $T = 0K$. The position swapping (c) in the *sandwich* profile occurs at $U_{11} = U_{22} = 0.05E_R$. (d-f) Shows the similar condensate density profiles for Cs-Rb TBEC with change in the interspecies interaction U_{12} at $T = 0K$. In this system the transition to *sandwich* geometry occurs at $U_{12}^c = 0.3E_R$.

1. *Third Goldstone mode in ^{87}Rb - ^{85}Rb TBEC*

To examine the mode evolution with the tuning of intraspecies interaction, we consider a quasi-1D TBEC consisting of ^{87}Rb and ^{85}Rb [28, 53]. In this system, we consider ^{87}Rb and ^{85}Rb as the first and second species, respectively. The axial trapping frequency for both the species is $\omega_z = 2\pi\times 80$ Hz with the anisotropy parameters along x and y directions as 12.33. The laser wavelength used to create the optical lattice potential is $\lambda_L = 775$ nm. The number of atoms are $N_1 = N_2 = 100$, which are confined in 100 lattice sites superimposed on harmonic potential. We choose the depth of the lattice potential $V_0 = 5E_R$ and set the tunneling matrix elements for the two species as $J_1 = 0.66E_R$ and $J_2 = 0.71E_R$, the intraspecies interaction U_{11} as $0.05E_R$ and the interspecies interaction U_{12} as $0.1E_R$. These set of DNLSE parameters are calculated by considering the width of the Gaussian beam as $0.3a$. Since the scattering length of ^{85}Rb is tunable with the Feshbach resonance [28], we study the excitation spectrum with the variation in U_{22}. The evolution of the Kohn mode functions with the variation of U_{22} is shown in Fig. 1. For $0.18 \leq U_{22} \leq 0.25E_R$, the system is in the miscible domain, and the Kohn mode is a linear combination of ^{87}Rb and ^{85}Rb Kohn modes. As we approach the phase separation by reducing the value of U_{22}, we observe a decrease in the ^{87}Rb component of the Kohn mode function amplitude and the mode component of ^{85}Rb goes soft at $0.062E_R$. The softening of the mode is evident from the evolution of the mode energies as shown in Fig. 2(a). The figure shows that the mode continues as the third Goldstone mode for $U_{22} \leq 0.062E_R$. The emergence of the third Goldstone mode is associated with a change in the geometry of the system, the density changes from overlapping to *sandwich* profile as shown in Figs. 3(a-c). Thus, as discussed in our earlier work [46], the binary condensate is separated into three distinct sub-components.

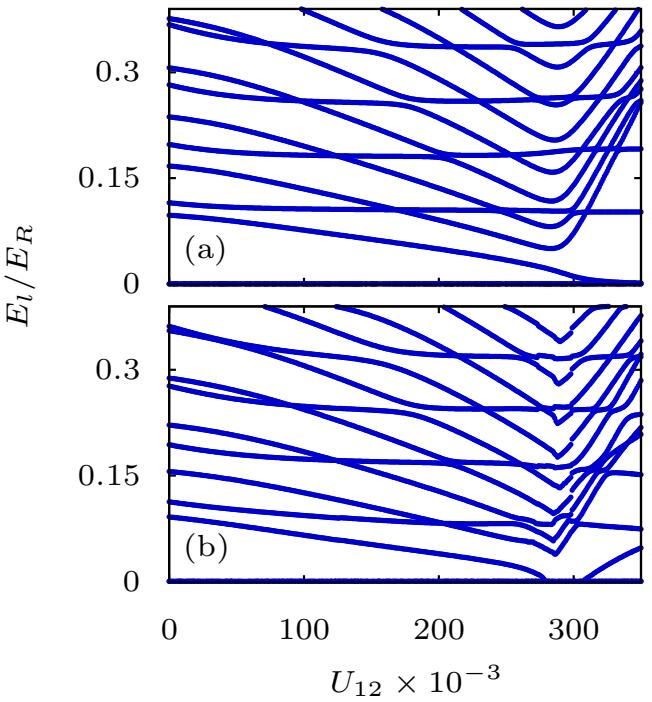

FIG. 4. The evolution of the energies of the low-lying modes as a function of the interspecies interaction in Cs-Rb (U_{12}) TBEC held in a quasi-1D lattice potential. (a) The excitation spectrum at $T = 0K$, and (b) excitation spectrum after including the quantum fluctuations. Here U_{12} is in units of the recoil energy E_R.

2. *Third Goldstone mode in ^{133}Cs - ^{87}Rb TBEC*

For mode evolution with the tuning of interspecies interaction, we consider the binary system of Cs-Rb [54, 55]. Here, we consider ^{133}Cs and ^{87}Rb as the first and second species, respectively. To study the modes evolution as the system undergoes transition from miscible to immiscible phase, the interspecies interaction U_{12} is varied, which is possible with magnetic Feshbach resonance [56]. The parameters of the system considered are $N_1 = N_2 = 100$ with the similar trapping frequencies as in the case of ^{87}Rb-^{85}Rb mixture. The lattice parameters are chosen as $J_1 = 0.92E_R, J_2 = 1.95E_R, U_{11} = 0.40E_R$, and $U_{22} = 0.21E_R$. At $U_{12} = 0$, the two condensates are uncoupled and have two Goldstone modes, one corresponding to each of the two species. At low values of U_{12}, in the miscible regime, the condensate density profile of both the species overlap as shown in Fig. 3(d). As we increase U_{12}, the Kohn mode of ^{87}Rb gradually goes soft and at a critical value U_{12}^c =$0.3E_R$ it is transformed into the third Goldstone mode. For $U_{12}^c < U_{12}$, the geometry of the condensate density profile changes and acquires *sandwich* structure in which the Cs condensate (higher mass) is at the center and flanked by Rb condensate (lower mass) at the edges as shown in Fig. 3(f). This is also evident from the evolution of the low-lying modes, shown in Fig. 4(a) and is reflected in the structural evolution of the quasiparticle amplitudes in Fig. 5. Hence the system attains an extra Goldstone mode after transition from miscible to *sandwich* type profile.

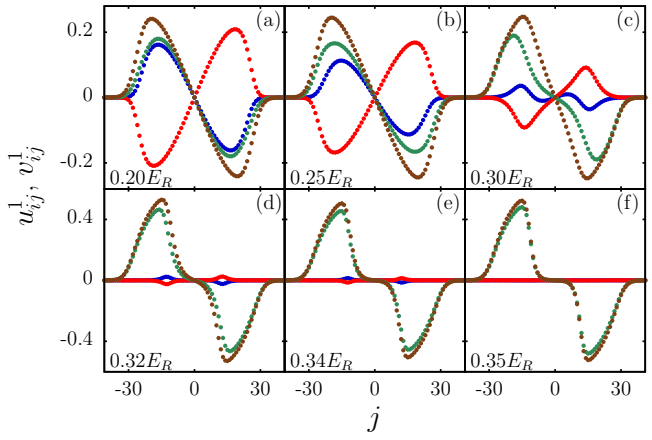

FIG. 5. The evolution of the quasiparticle amplitudes corresponding to the Kohn mode as the interspecies interaction is increased from $0.2E_R$ to $0.35E_R$ for Cs-Rb TBEC in quasi-1D lattice potential at $T = 0K$. (a-c) In miscible regime, the Kohn mode has contributions from both the species. (d-f) For $U_{22} > 0.3E_R$ the Kohn mode of ^{87}Rb goes soft, whereas that of ^{133}Cs decreases in amplitude.

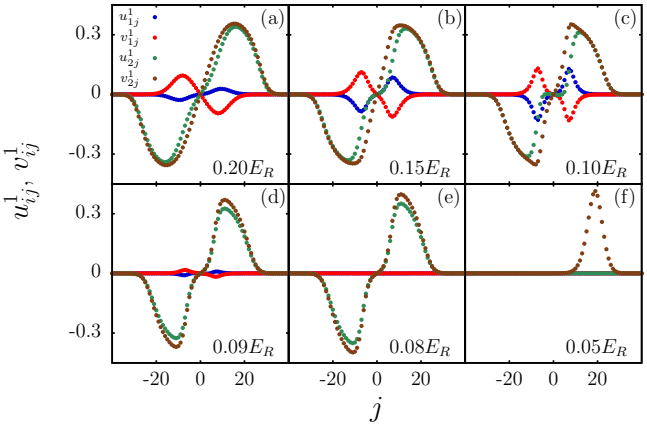

FIG. 6. The evolution of the quasiparticle amplitudes corresponding to the Kohn mode for ^{87}Rb-^{85}Rb TBEC in the presence of the fluctuations as the intraspecies interaction of ^{85}Rb (U_{22}) is decreased from $0.2E_R$ to $0.05E_R$. (a-e) The Kohn mode of ^{85}Rb goes soft, whereas that of ^{87}Rb is decreases in amplitude and finally vanishes in (e). (f) The sloshing mode, which emerges after phase separation as the *sandwich* density profile transforms into *side-by-side* profile.

3. *Position swapping of species*

A remarkable feature in the evolution of the condensate density profiles of ^{87}Rb-^{85}Rb TBEC with the variation of U_{22} is the observation of the position swapping in the immiscible domain. This is absent when the trapping potential consists of only the harmonic potential (continuous system), and is the result of the discrete symmetry associated with the optical lattice. As discussed earlier, in this system, we fix U_{11} and U_{12}, and vary U_{22} (intraspecies interaction of ^{85}Rb). At higher values of U_{22} the TBEC is in the miscible phase, and as we decrease U_{22}, at the critical value $U_{22}^c = 0.17E_R$ the TBEC enters the immiscible domain. The geometry of the density profiles is *sandwich* type and the component with smaller U_{ii} is at the centre. An example of condensate density profile in this domain, $U_{22} = 0.06E_R$, is shown in Fig. 3(b). In the figure, the species with smaller intraspecies interaction (^{87}Rb) is at the center and ^{85}Rb is at the edges. As U_{22} is further decreased, the system continues to be in the same phase. During evolution, an instability arises when both intraspecies interactions are same ($U_{11} = U_{22} = 0.05$). At this value of U_{22} the components swap their places in the trap. This is also reflected in the excitation spectrum, a discontinuity at $U_{22} = 0.05E_R$ in the plot of mode evolution shown in Fig. 2(a) is a signature of the instability. On further decrease of U_{22}, we enter the $U_{22} < U_{11}$ domain and ^{85}Rb occupies the center of the trap. An example of density profiles in this domain, $U_{22} = 0.03$ is shown in Fig. 3(c). The position swapping, however, does not occur in Cs-Rb system as in that case we vary U_{12}.

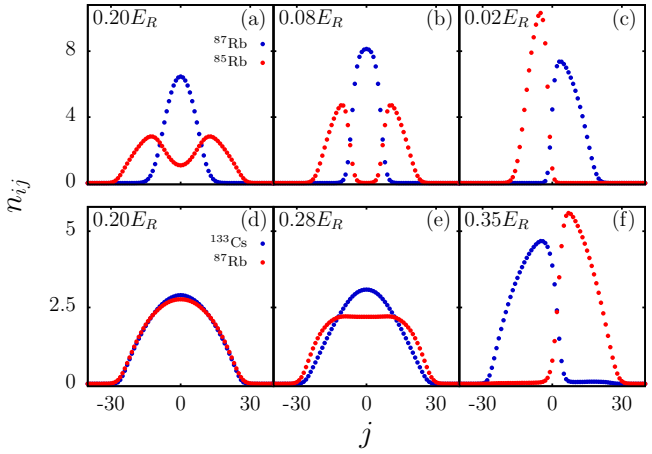

FIG. 7. The fluctuation induced transition in the geometry of the total density profile (condensate + quantum fluctuations) of TBEC at $T = 0K$ in quasi-1D lattice potential. (a-c) The transition in ^{87}Rb-^{85}Rb system from miscible to *sandwich* and finally in the *side-by-side* profile with the change in the intraspecies interaction. (d-e) The transition in Cs-Rb TBEC from miscible to *side-by-side* profile with the change in interspecies interaction U_{12}. The geometry of the ground state of both system in the immiscible regime is different from that at zero temperature in the absence of the fluctuations Fig.3.

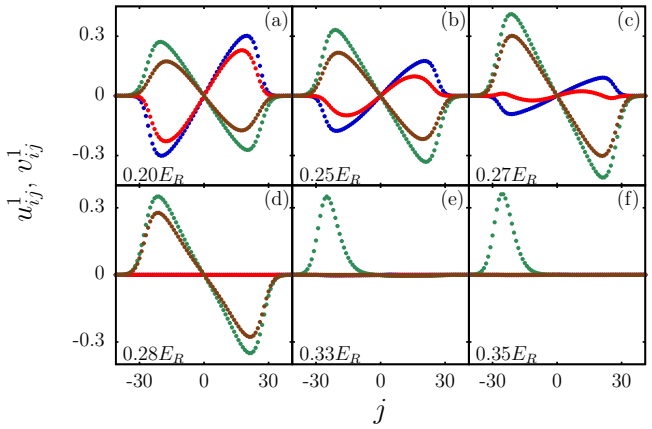

FIG. 8. The evolution of the quasiparticle amplitude corresponding to the Kohn mode for Cs-Rb TBEC in the presence of fluctuations as (a-d)The Kohn mode evolves as the interspecies interaction is increased. (e-f) It is transformed into a sloshing mode as the TBEC acquires *side-by-side* density profile after phase separation.

C. Effect of quantum fluctuations

We compute the condensate profiles and modes for ^{87}Rb-^{85}Rb TBEC, however, include the effect of quantum fluctuations. We, then, encounter severe oscillations in the number of atoms during iterations to solve the DNLSEs and there is no convergence. To mitigate this, we use successive under-relaxation technique with $r^{\rm un} = 0.6$. For computations, we consider the same set of parameters as in the case of $T = 0K$ without fluctuations. The fluctuations break the spatial symmetry of the system as we vary the intraspecies interaction of ^{85}Rb (U_{22}). In the immiscible domain, the condensate density profile changes from *sandwich* to *side-by-side* profile at $0.078E_R$. The system acquires a new stable ground state as the chemical potential of the system decreases from $0.92E_R$ to $0.80E_R$. The evolution of the mode energies with U_{22} including the fluctuation is shown in Fig. 2(b). It is evident that at this value $U_{22} = 0.078E_R$, the ^{85}Rb Kohn mode goes soft and emerges as a sloshing mode. The transformations in the mode functions as U_{22} is decreased about this point are shown in Fig. 6. This topological phase transition is evident from the density profiles of the TBEC in the presence of the quantum fluctuations as shown in Fig. 7(a-c).

In the Cs-Rb system, due to quantum fluctuations, the Kohn mode of ^{87}Rb goes soft at a lower value of U_{12} compared to the value without fluctuations. This is evident in the mode evolution with quantum fluctuations as shown in Fig. 4(b). The discontinuity in the spectrum is the signature of the transition from miscible to immiscible regime. The soft Kohn mode gains energy and gets hard at $0.31E_R$. This mode hardening is due to the topological change in the ground state density profile from miscible to the *side-by-side* profile, shown in Fig. 7(d-f). The lowest mode with nonzero excitation energy corresponding to the *side-by-side* profile is shown in Fig. 8(e-f).

V. CONCLUSIONS

We have studied the ground state density profiles and the excitation spectrum of TBEC in quasi-1D optical lattices. We observe that the system gains an additional Goldstone mode at phase-separation at zero temperature. Furthermore, in TBEC where miscible to immiscible transition driven through the variation of the intraspecies interaction (^{87}Rb-^{85}Rb), a finite discontinuity in the excitation energy spectra is observed in the neighbourhood of equal intraspecies interaction strengths. In the presence of quantum fluctuations, on varying the intraspecies interaction of ^{85}Rb, in the immiscible regime, the ground state density profiles transform from *sandwich* to *sie-by-side* geometry. This is characterized by the hardening of the Kohn mode which emerges as a sloshing mode. The fluctuation induced topological change from completely miscible to *side-by-side* ground state density profile is also evident in ^{133}Cs-^{87}Rb mixture. Our current studies show that the geometry of the density profiles with and without quantum fluctuations are different. Since quantum fluctuations are present in experiments, it is crucial to include quantum fluctuations to obtain correct density profiles of TBECs in optical lattices in the phase-separated domain.

ACKNOWLEDGMENTS

We thank S. Gautam and S. Chattopadhyay for useful discussions. The results presented in the paper are based on the computations using the 3TFLOP HPC Cluster at Physical Research Laboratory, Ahmedabad, India.

[1] M. A. Cazalilla, R. Citro, T. Giamarchi, E. Orignac, and M. Rigol, Rev. Mod. Phys. **83**, 1405 (2011).
[2] E. H. Lieb and W. Liniger, Phys. Rev. **130**, 1605 (1963).
[3] O. Morsch and M. Oberthaler, Rev. Mod. Phys. **78**, 179 (2006).
[4] I. Bloch, J. Dalibard, and W. Zwerger, Rev. Mod. Phys. **80**, 885 (2008).
[5] S. Friebel, C. D'Andrea, J. Walz, M. Weitz, and T. W. Hänsch, Phys. Rev. A **57**, R20 (1998).
[6] L. Guidoni and P. Verkerk, Phys. Rev. A **57**, R1501 (1998).
[7] B. Paredes, A. Widera, V. Murg, O. Mandel, S. Folling, I. Cirac, G. V. Shlyapnikov, T. W. Hansch, and I. Bloch, Nature **429**, 277281 (2004).
[8] I. Bloch, Nat Phys **1**, 2330 (2005).
[9] S. Sachdev, *Quantum Phase Transitions* (Cambridge University Press, 2011).
[10] M. Greiner, O. Mandel, T. Esslinger, T. W. Hansch, and I. Bloch, Nature **415**, 3944 (2002).
[11] H. Moritz, T. Stöferle, M. Köhl, and T. Esslinger, Phys. Rev. Lett. **91**, 250402 (2003).
[12] T. Stöferle, H. Moritz, C. Schori, M. Köhl, and T. Esslinger, Phys. Rev. Lett. **92**, 130403 (2004).
[13] B. L. Tolra, K. M. O'Hara, J. H. Huckans, W. D. Phillips, S. L. Rolston, and J. V. Porto, Phys. Rev. Lett. **92**, 190401 (2004).
[14] C. Orzel, A. K. Tuchman, M. L. Fenselau, M. Yasuda, and M. A. Kasevich, Science **291**, 2386 (2001).
[15] M. Greiner, I. Bloch, O. Mandel, T. W. Hänsch, and T. Esslinger, Phys. Rev. Lett. **87**, 160405 (2001).
[16] C. Fort, F. S. Cataliotti, L. Fallani, F. Ferlaino, P. Maddaloni, and M. Inguscio, Phys. Rev. Lett. **90**, 140405 (2003).
[17] C. D. Fertig, K. M. O'Hara, J. H. Huckans, S. L. Rolston, W. D. Phillips, and J. V. Porto, Phys. Rev. Lett. **94**, 120403 (2005).
[18] L. Fallani, L. De Sarlo, J. E. Lye, M. Modugno, R. Saers, C. Fort, and M. Inguscio, Phys. Rev. Lett. **93**, 140406 (2004).
[19] S. Burger, F. S. Cataliotti, C. Fort, F. Minardi, M. Inguscio, M. L. Chiofalo, and M. P. Tosi, Phys. Rev. Lett. **86**, 4447 (2001).
[20] F. S. Cataliotti, S. Burger, C. Fort, P. Maddaloni, F. Minardi, A. Trombettoni, A. Smerzi, and M. Inguscio, Science **293**, 843 (2001).
[21] M. Krämer, C. Menotti, L. Pitaevskii, and S. Stringari, Eur. Phys. J. D **27**, 247261 (2003).
[22] E. Lundh, Phys. Rev. A **70**, 033610 (2004).
[23] J.-P. Martikainen and H. T. C. Stoof, Phys. Rev. A **68**, 013610 (2003).
[24] A. M. Rey, G. Pupillo, C. W. Clark, and C. J. Williams, Phys. Rev. A **72**, 033616 (2005).
[25] A. M. Rey, *Ultracold bosonic atoms in optical lattices*, Ph.D. thesis, University of Maryland, USA (2004).
[26] M. P. A. Fisher, P. B. Weichman, G. Grinstein, and D. S. Fisher, Phys. Rev. B **40**, 546 (1989).
[27] R. Navarro, R. Carretero-González, and P. G. Kevrekidis, Phys. Rev. A **80**, 023613 (2009).
[28] S. B. Papp, J. M. Pino, and C. E. Wieman, Phys. Rev. Lett. **101**, 040402 (2008).
[29] S. Tojo, Y. Taguchi, Y. Masuyama, T. Hayashi, H. Saito, and T. Hirano, Phys. Rev. A **82**, 033609 (2010).
[30] S. Gautam and D. Angom, J. Phys. B **44**, 025302 (2011).
[31] S. Gautam and D. Angom, Phys. Rev. A **81**, 053616 (2010).
[32] T. Kadokura, T. Aioi, K. Sasaki, T. Kishimoto, and H. Saito, Phys. Rev. A **85**, 013602 (2012).
[33] C. Ticknor, Phys. Rev. A **88**, 013623 (2013).
[34] D. Gordon and C. M. Savage, Phys. Rev. A **58**, 1440 (1998).
[35] J. Catani, L. De Sarlo, G. Barontini, F. Minardi, and M. Inguscio, Phys. Rev. A **77**, 011603 (2008).
[36] B. Gadway, D. Pertot, R. Reimann, and D. Schneble, Phys. Rev. Lett. **105**, 045303 (2010).
[37] G.-H. Chen and Y.-S. Wu, Phys. Rev. A **67**, 013606 (2003).
[38] A. B. Kuklov and B. V. Svistunov, Phys. Rev. Lett. **90**, 100401 (2003).
[39] A. Kuklov, N. Prokof'ev, and B. Svistunov, Phys. Rev. Lett. **92**, 050402 (2004).
[40] M.-C. Cha, Int. J. Mod. Phys. B **27**, 1362002 (2013).
[41] F. Zhan and I. P. McCulloch, Phys. Rev. A **89**, 057601 (2014).
[42] T. Mishra, R. V. Pai, and B. P. Das, Phys. Rev. A **76**, 013604 (2007).
[43] Y.-C. Kuo and S.-F. Shieh, J. Math. Anal. Appl. **347**, 521 (2008).
[44] J. Ruostekoski and Z. Dutton, Phys. Rev. A **76**, 063607 (2007).
[45] A. Griffin, Phys. Rev. B **53**, 9341 (1996).
[46] A. Roy, S. Gautam, and D. Angom, Phys. Rev. A **89**, 013617 (2014).
[47] A. Roy and D. Angom, Phys. Rev. A **90**, 023612 (2014).
[48] M. L. Chiofalo, M. Polini, and M. P. Tosi, Eur. Phys. J. D **11**, 371 (2000).
[49] D. Jaksch, C. Bruder, J. I. Cirac, C. W. Gardiner, and P. Zoller, Phys. Rev. Lett. **81**, 3108 (1998).
[50] G. Baym and C. J. Pethick, Phys. Rev. Lett. **76**, 6 (1996).
[51] E. Anderson, Z. Bai, C. Bischof, S. Blackford, J. Demmel, J. Dongarra, J. D. Croz, A. Greenbaum, S. Hammarling, A. McKenney, and D. Sorensen, *LAPACK Users' Guide*, 3rd ed. (Society for Industrial and Applied Mathematics, Philadelphia, PA, 1999).
[52] T. P. Simula, S. M. M. Virtanen, and M. M. Salomaa, Comp. Phys. Comm. **142**, 396 (2001).
[53] S. Händel, T. P. Wiles, A. L. Marchant, S. A. Hopkins, C. S. Adams, and S. L. Cornish, Phys. Rev. A **83**, 053633 (2011).

[54] D. J. McCarron, H. W. Cho, D. L. Jenkin, M. P. Köppinger, and S. L. Cornish, Phys. Rev. A **84**, 011603 (2011).

[55] A. Lercher, T. Takekoshi, M. Debatin, B. Schuster, R. Rameshan, F. Ferlaino, R. Grimm, and H.-C. Ngerl, Eur. Phys. J. D **65**, 3 (2011).

[56] K. Pilch, A. D. Lange, A. Prantner, G. Kerner, F. Ferlaino, H.-C. Nägerl, and R. Grimm, Phys. Rev. A **79**, 042718 (2009).